PHYSICAL PROPERTIES OF INCOMPLETELY COMPACTED EQUILIBRATED ORDINARY CHONDRITES: IMPLICATIONS FOR ASTEROIDAL STRUCTURE AND IMPACT PROCESSING.

Matthew R. Sasso[1], Robert J. Macke[2], Daniel T. Britt[2], Mark L. Rivers[3], Denton S. Ebel[4], Jon M. Friedrich[1,4], [1]Department of Chemistry, Fordham University, Bronx, NY 10458, [2]Department of Physics, University of Central Florida, Orlando, FL 32816, [3]Consortium for Advanced Radiation Sources, University of Chicago, Argonne, IL 60439, [4]Department of Earth and Planetary Sciences, American Museum of Natural History, New York, NY 10024.

Introduction: Aside from robotic exploration, meteorites are our primary source of information about the asteroids that they sample. Although there are some discrepancies, there are dynamical [1], spectral [2], and compositional [3,4] evidence for an S-type asteroid connection to the ordinary chondrite meteorites. Reconciling the measured bulk density of chondrites with that of asteroids can yield important inferences about the internal structure of asteroids [5]. For example, the bulk density of S-type asteroids is typically much less than the bulk density of chondrites, leading to the inference that asteroids contain a significant quantity of macroporosity.

We have identified several unusual ordinary chondrites that have been incompletely compacted relative to petrologically similar but much less porous chondrites [e.g. 6]. Although these are equilibrated chondrites, they have extreme amounts of pore spaces between mineral grains. Here, we detail our efforts quantifying the nature of the pore spaces in these chondrites and we examine the implications for the structure and mechanical processing of the asteroids from which these chondrites originate. Our pore size distribution data may also provide constraints for the modeling of heat flow and shock waves within primordial chondritic parent bodies.

Samples and Methods: We examined portions of Miller (Arkansas) (H5), Mount Tazerzait (L5), NWA 2380 (LL5), Sahara 98034 (H5), and Tjerebon (L5). To examine the physical properties of this suite of ordinary chondrites, we used a combined He pycnometry/Archimedean bead volumetric method, and synchrotron x-ray microtomography (μCT). Typical chondrite-related data collection details for each method can readily be found in [6-8]. From He pycnometry, we obtain information about total porosity. Sample volume was quantified with the Archimedean bead method and/or μCT. Our μCT measurements allow rigorous 3D quantification of individual pores, Fe(Ni) metal, and Fe(Ni)S sulfide volumes and their spatial distribution without the sample preparation artifacts inherent to thin sectioning. We used two resolutions for our μCT measurements: 8.3 and 16.6 μm/voxel. To extract quantitative data from our μCT image stacks, we used BLOB3D [9]. Our separations yielded minimum isolatable volumes of 3.41×10^{-6} and 2.72×10^{-5} mm^3 for high and low resolution data respectively. Here, we will focus on a detailed analysis of size distributions of voids in our samples.

Figure 1. Typical tomograms of two incompletely compacted equilibrated ordinary chondrites. The brightest Fe(Ni) metal grains can easily be differentiated from the slightly darker Fe(Ni)S materials. Significant void spaces (represented in black) between dark grey silicate grains can also easily be identified. Samples are completely surrounded by air (black).

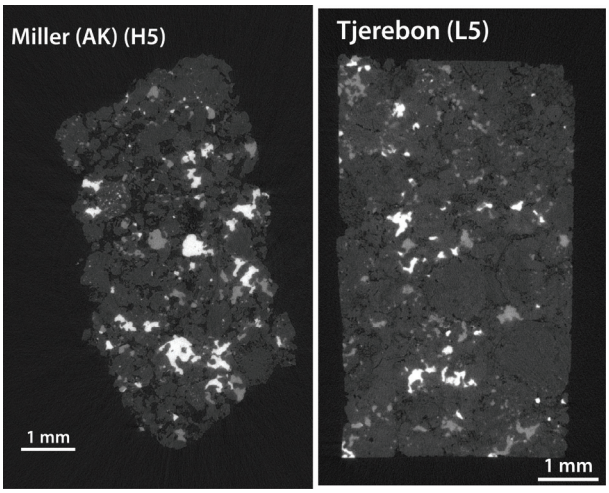

Results: Not surprisingly, each of these uncompacted ordinary chondrites have bulk densities lower than those of typical ordinary chondrites of the same chemical class. For example, Tjerebon, the most compacted chondrite in our suite has a bulk density of 3.11 g/cm^3, only ~7% lower than a typical L chondrite, while Miller the least compacted, has a bulk density of 2.98 g/cm^3, nearly 13% lower than a typical H chondrite [5]. Our determined bulk densities of other chondrites in our suite are noted below.

Before we begin a discussion of size resolved void volume results within our chondrites, we need to clarify a distinction between the visible porosity , which in our case is μCT resolution dependent, and "total" porosity, which we take as the result of our He pycnometry measurements. We compare these values (low resolution μCT versus high resolution μCT versus He

pycnometry) in discussing the quantity of pores visible within our samples at differing resolutions, which can give us a picture of the pore size distribution. As expected, in each case, 16.6 µm/voxel µCT data yields less visible porosity than 8.3 µm/voxel µCT data which in turn is less than the "total" porosity.

Low resolution µCT data for Miller (Fig. 1) demonstrated observable porosity comprising 10.1% of the sample. Visible porosity increases to 14.3% at 8.3 µm/voxel and the He pycnometry method yields 20.0% porosity.

Mount Tazerzait data contained similar patterns for differing resolutions and methods. Low resolution µCT Mount Tazerzait results gave a visible pore volume of 4.43% while data collected at higher resolution produced a visible porosity of 8.03%. In this case, the measured "total" porosity 12.6%, which is 54% greater than the total quantity of voids detectable by high resolution µCT alone (Fig. 2). The same sample of Mount Tazerzait yielded a bulk density of 3.18 g/cm^3.

Figure 2. Cumulative distribution of total pore volumes in Mount Tazerzait (L5) as quantified by µCT and He pycnometry. Individual pore volumes were isolated for low resolution (16.6 µm/voxel) µCT data.

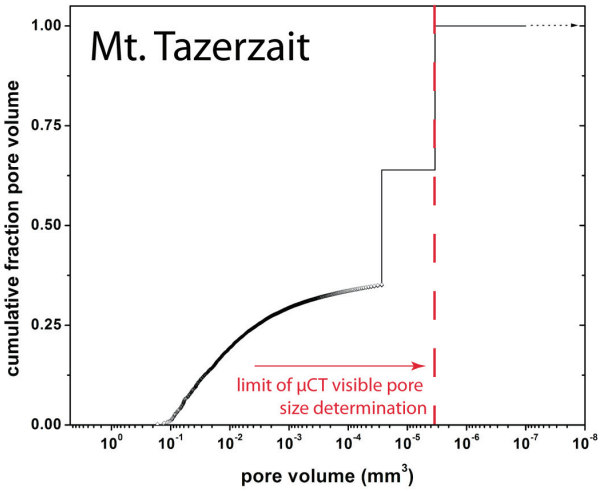

We determined the total porosity NWA 2380 to be 18.7%. Low µCT resolution data for NWA 2380 sample 1 gave a detectable porosity of 6.49% while high resolution µCT produced a visible porosity of 10.6%. The bulk density of NWA 2380 is 2.82 g/cm^3.

The sum total of void spaces for low resolution µCt data in Sahara 98034 demonstrated a porosity of 3.83%, while the total visible pore volume of Sahara 98034 more than doubles to 7.82% with the use of high resolution µCT. He pycnometry measurements gave a porosity of 16.1 ± 2.0%. Sahara 98034's bulk density is 2.91 g/cm^3.

In the case of Tjerebon (Fig. 1), the total porosity visible with low resolution µCT data only amounts to a volume of 0.62% of the meteorite. Using our high resolution data, the volume of detectable voids jumps to 3.52% porosity. A very reproducible total porosity of 9.82% was determined with He pycnometry.

Discussion and Conclusions: Distinct mineral grains and the interstitial pores between them demonstrate the incomplete compaction experienced by these chondrites (Fig.1). We have rigorously quantified the size-volume relationships of the porosity in these samples (e.g. Fig. 2). When the µCT visible pores are subtracted from the total porosity, the resulting porosities are extremely similar to those of compacted chondrites [5] indicating that significant amounts of microcracks are present (Fig. 2). These microcracks probably originated from impact processing that was intense enough to indurate, but not completely compact the target materials [5,8].

The majority of chondrites have lower porosities than the samples investigated here. However, if their parent asteroids actually contain significant fractions of high porosity, incompletely compacted chondritic material, the asteroidal macroporosity necessary to account for the discrepancy with chondritic porosity may be lower than previously thought. Additionally, the materials investigated here come from at least three chemically distinct parent bodies indicating that incomplete compaction is not a limited occurrence within the asteroid belt.

Our initial investigations of total metal content and metal grain size number distributions, as determined by µCT, suggest these samples were metamorphosed in their current arrangement. Further data, such as detailed noble gas and mineral closure data may help place these samples into a temporal context.

References: [1] Wetherill G. W. (1985) *Meteoritics, 20,* 1-22. [2] Gaffey M. J. et al. (1993) *Icarus, 106*, 573-602. [3] McCoy T. J. et al. (2001) *Meteoritics & Planet. Sci., 36,* 1661-1672. [4] Nittler L. R. et al. (2001) *Meteoritics & Planet. Sci., 36,* 1673-1695. [5] Consolmagno G. J. et al. (2008) *Chemie der Erde, 68,* 1-29. [6] Friedrich J. M. et al. (2008) *Planet. Space Sci., 56,* 895-900. [7] Consolmagno G. J. and Britt D. T. (1998) *Meteoritics & Planet. Sci., 33,* 1231-1241. [8] Friedrich J. M. et al. (2008) *Earth Planet. Sci. Lett., 275,* 172-180. [9] Ketcham R. A. (2005) *Geosphere, 1,* 32–41.